

516
LA-UR-08-1264

Approved for public release;
distribution is unlimited.

Title: A MATERIAL INTERFACE TRANSITION ALGORITHM
FOR MULTIPHASE FLOW

Author(s): MM FRANCOIS
RB LOWRIE
ED DENDY

Intended for: Proceedings of
2008 ASME FLUIDS ENGINEERING CONFERENCE
JACKSONVILLE, FLORIDA, USA



Los Alamos National Laboratory, an affirmative action/equal opportunity employer, is operated by the Los Alamos National Security, LLC for the National Nuclear Security Administration of the U.S. Department of Energy under contract DE-AC52-06NA25396. By acceptance of this article, the publisher recognizes that the U.S. Government retains a nonexclusive, royalty-free license to publish or reproduce the published form of this contribution, or to allow others to do so, for U.S. Government purposes. Los Alamos National Laboratory requests that the publisher identify this article as work performed under the auspices of the U.S. Department of Energy. Los Alamos National Laboratory strongly supports academic freedom and a researcher's right to publish; as an institution, however, the Laboratory does not endorse the viewpoint of a publication or guarantee its technical correctness.

FEDSM 2008-55304

A MATERIAL INTERFACE TRANSITION ALGORITHM FOR MULTIPHASE FLOW¹

Marianne M. Francois
Los Alamos National Laboratory
Computational Physics Group
Los Alamos, NM 87545, USA
mmfran@lanl.gov

Robert B. Lowrie
Los Alamos National Laboratory
Computational Physics Group
Los Alamos, NM 87545, USA
lowrie@lanl.gov

Edward D. Dendy
Los Alamos National Laboratory
Computational Analysis and Simulation Group
Los Alamos, NM 87545, USA
dendy@lanl.gov

LA-UR-08-1264

ABSTRACT

Volume tracking method, also referred to as the volume-of-fluid (VOF) method introduces "numerical surface tension" that breaks a filament into a series of droplets whenever the filament is under-resolved. Adaptive mesh refinement can help avoid under-resolution, but a fully-developed flow will still generate filaments that cannot be resolved without enormous computational cost. We propose a complementary new approach that consists of transitioning to a continuous interface representation (i.e. without interface reconstruction) in regions of under-resolved interfacial curvature where volume tracking has become erroneous. The price of the continuous interface treatment is a small amount of numerical mass diffusion, even if the physical interface is immiscible. However, we have found that for certain measures, the overall accuracy is greatly improved by using our transitioning algorithm. The algorithm is developed in the context of the single fluid formulation of the incompressible Navier-Stokes equations. Numerical

standard vortices advection test cases and Rayleigh-Taylor instability computations are presented to illustrate the transition algorithm potential.

INTRODUCTION

Volume-of-fluid (VOF) method, also referred to as volume tracking method (Rider and Kothe, 1998), is a broadly used numerical method to simulate immiscible multiphase flow in which the interface is represented as a sharp boundary and is being evolved as part of the solution of the flow equations. The interface is not explicitly tracked but is captured by the material volume fraction. In volume tracking, as in front-tracking and level-set methods, a single field formulation is employed, i.e. there is a single velocity field and the fluid properties, such as density and viscosity, are averaged in the mixed cells based on material volume fractions. In the volume tracking method of Rider and Kothe (1998), the interface is geometrically reconstructed by piecewise linear interface planes (PLIC)

¹ By acceptance of this paper, the publisher recognizes that the U.S. Government retains a nonexclusive, royalty-free license to publish or reproduce the published form of this contribution, or to allow others to do so, for U.S. Government purposes.

within each mixed cell to accurately compute the mass and momentum fluxes. The method's main drawback is when the interface reconstruction becomes under-resolved, i.e. when the interface length scale becomes smaller than 3 to 4 grid points. Interface reconstruction is known to introduce "numerical surface tension" that breaks a filament into a series of droplets whenever the filament is under-resolved (Rider and Kothe, 1998). Adaptive mesh refinement can help avoid under-resolution, but a fully-developed flow will still generate filaments that cannot be resolved without enormous computational cost. Another approach is to improve the interface reconstruction method. Dyadechko and Shashkov (2005) have developed a more accurate way of reconstructing the interface from volume fractions by introducing the first moment information. However their method still breaks thin filaments structure into small fluid pieces although it occurs at lower resolution. Therefore, we propose herein a complementary new approach that consists of transitioning from volume tracking to a continuous interface representation (i.e. without interface reconstruction) in regions where volume tracking has become erroneous.

Cerne et al. (2001) have coupled a volume-of-fluid method to a two-fluid formulation and devised an empirical switching criteria based on a dispersion coefficient obtained from the volume fractions. In this work, we only consider a single fluid formulation and we base the switch criteria on the interfacial curvature, a geometric measure.

COMPUTATIONAL FORMULATION

In this work, the volume fractions, denoted by f , are evolved by the following equation:

$$\frac{\partial f}{\partial t} + \vec{u} \cdot \nabla f = 0 \quad (1)$$

This equation is also referred to the volume fraction advection equation. For a fluid flow simulation, this equation is solved in addition to the mass and momentum conservation equations. In volume tracking method, Equation (1) is solved by geometrically reconstructing interface planes. Other approaches consist of solving Equation (1) with high-order numerical methods.

In this work, for volume tracking (VOF) we reconstruct the interface by piecewise linear planes (PLIC) as in Rider and Kothe (1998) in order to estimate the advection fluxes. This ensures a sharp interface representation of the interface without numerical diffusion. For the continuous interface representation, we employ the interface preserver (IP) approach of Dendy and Rider (2004), also known as the artificial steepening or compressive limiter method, in which the single material contact steepener of Yang (1990) is extended to material interfaces. In IP, the volume fraction gradients are steepened in order to keep the mass diffusion to a minimum.

Our material interface transition algorithm is the following. Initially, all full and mixed cells are flagged as VOF cells. Then at every time step, curvature is estimated in interfacial cells

using the height function method as presented in Francois et al. (2006) and Cummins et al. (2005). If the curvature is higher than a certain value (meaning that the interface reconstruction will be poor or will be broken), then the cell is flagged as an IP cell. This criterion is based on our previous findings that suggested that the height function method is best when the curvature multiplied by the mesh spacing is smaller than about 1/5 (Cummins et al. 2005). The advection flux is computed on each cell face either by VOF or IP depending on the cell flag and velocity direction. And finally volume fractions are updated in time. Any overshoots or undershoots are corrected to ensure mass conservation.

NUMERICAL ADVECTION TEST CASES

In this section, we present common numerical advection test case to test our transition algorithm.

Single vortex deformation flow field

The test case of a single vortex deformation flow field is a common test case used for testing material advection algorithms. Initially a circular interface of radius 0.15 is located at (0.5, 0.75) in a unit square domain. The velocity field (u_x , u_y) is specified on the entire domain as:

$$\begin{aligned} u_x &= \sin^2(\pi x) \sin(2\pi y) \cos\left(\frac{\pi t}{T}\right) \\ u_y &= -\sin^2(\pi y) \sin(2\pi x) \cos\left(\frac{\pi t}{T}\right) \end{aligned} \quad (2)$$

where x and y are the spatial coordinates, and t is the time coordinate and T is the time period and is taken as 8 for this test case. The simulation is run on a 32×32 mesh and until $T/2$ the time at which the maximum stretching occur. We use a constant time step based on a CFL number of 0.1 and a maximum velocity of unity.

The volume fractions contours are shown in Figure 2 at time $t=2$. Note that for the VOF method the interface planes are not plotted but the volume fraction contours are rather plotted to facilitate the comparison with the IP and transition algorithm methods. We observe that on the 32×32 mesh (1) the VOF algorithm leads to the breaking of the interface into droplets, (2) the IP interface slightly diffuses the interfaces but keeps the correct interface topology and (3) the transition algorithm avoids the interface break-up.

In order to quantify our results, we define an error metric as a function of time to measure the advection error on the coarse mesh (32×32) with respect to the fine mesh reference solution (512×512). The error metric, denoted by δ and similar to the one in Cerne et al. (2001) is defined as:

$$\delta(t) = \frac{1}{V_f} \frac{1}{N_i N_j} \sum_{i,j} \left(|f_{i,j}(t) - f_{i,j}^{ref}(t)|^2 \right) \quad (3)$$

where N are the number of points in the each direction, $f_{i,j}$ are the volume fractions at each cell, V_f is the volume of the material being advected. The error δ is plotted in Figure 1 for VOF, IP and the transition algorithm. This plot shows that the

overall accuracy is greatly improved by using our material interface transition algorithm. At early times (from $t=0$ to $t=2$), VOF is more accurate than IP and then after $t=2$ IP is more accurate than VOF. The error using our transition algorithm which is based on a curvature switch criterion minimizes the overall error.

To investigate the order of accuracy of the transition algorithm, we perform a mesh resolution study. We consider three mesh sizes: 32×32 , 64×64 and 128×128 . The volume fraction contours for the 64×64 and 128×128 meshes are shown in Figure 3 and Figure 4, respectively. As the mesh is refined, the interface breaks at later times compared to the coarse mesh case with the VOF method.

The error metric δ is plotted versus time in Figure 5 for all meshes and interface representation methods. As the mesh is refined the global error decreases as expected for all methods. The global error using VOF on the finer mesh is the smallest compared to IP and the transition algorithm, since the interface break-up appears at later times and is localized to a smaller part in the computational domain. The advantage of the transition algorithm is clearly seen on the coarser mesh. The error is shown as a function of the mesh spacing in Figure 6. The IP method is shown to be first-order accurate and the VOF method is shown to be second-order accurate, as expected. The transition algorithm is shown to follow the second-order accurate behaviour as the mesh is refined, which is a nice feature of our algorithm. In terms of computational time, the new algorithm is comparable to the volume tracking and interface preserver methods on the same mesh size.

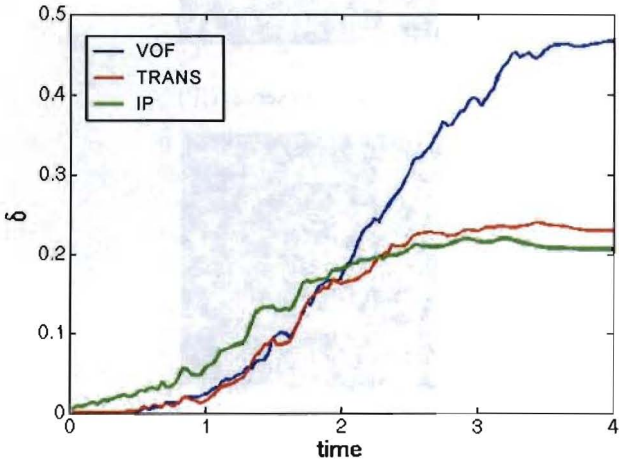
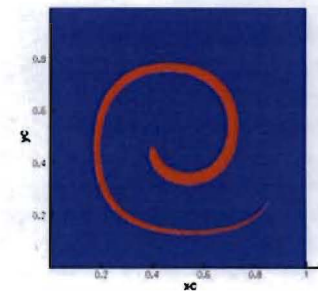
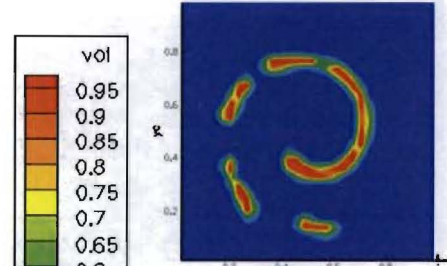


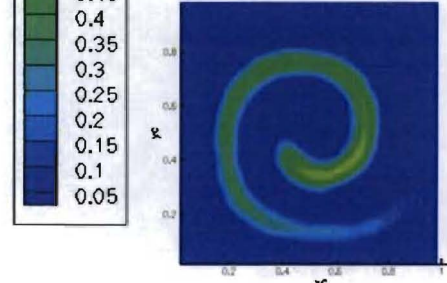
Figure 1: Volume fraction error versus time for the single vortex deformation flow field of period $T=8$ on a 32×32 mesh. The reference solution is obtained on a 512×512 mesh.



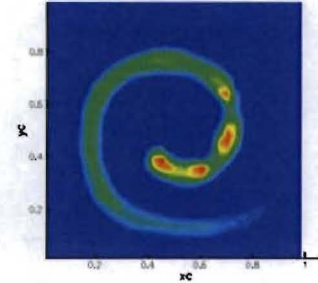
(a) Reference volume tracking solution on a 512×512 mesh



(b) Volume tracking (VOF)

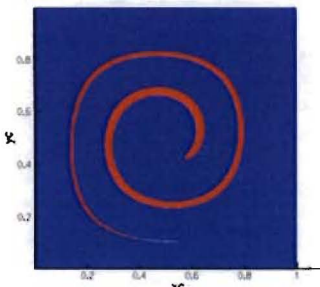


(c) Interface preserver (IP)

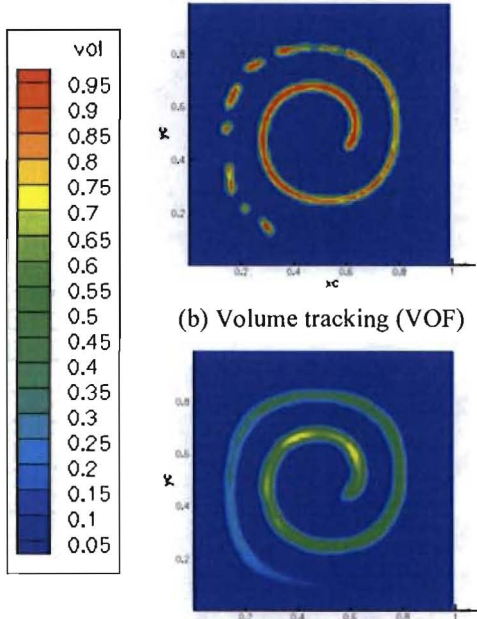


(d) Transition algorithm (TRANS)

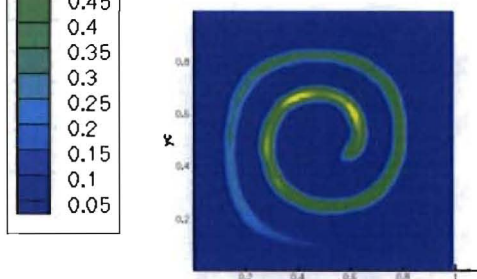
Figure 2: Volume fraction contours at time $t=2$ for the single vortex deformation flow field of period $T=8$ on a 32×32 mesh; (a) reference volume tracking solution on a 512×512 mesh, (b) volume tracking, (c) interface preserver and (d) transition algorithm.



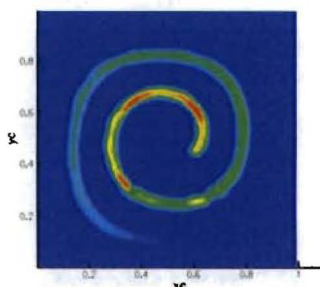
(a) Reference volume tracking solution on a 512×512 mesh



(b) Volume tracking (VOF)

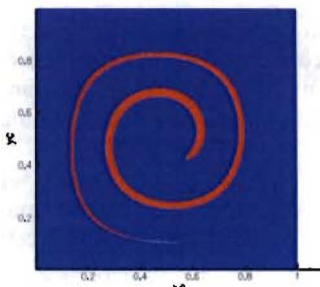


(c) Interface preserver (IP)

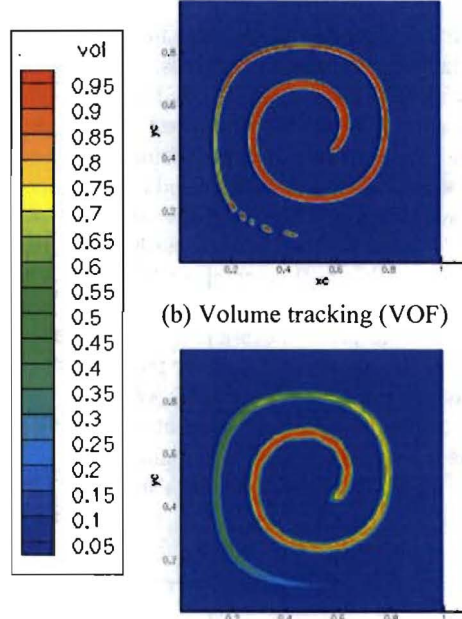


(d) Transition algorithm (TRANS)

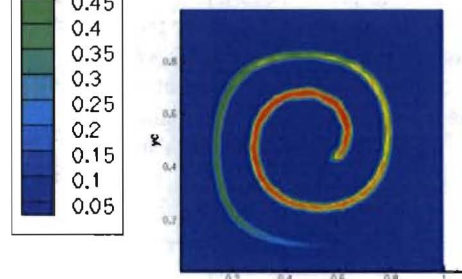
Figure 3: Volume fraction contours at time $t=4$ for the single vortex deformation flow field of period $T=8$ on a 64×64 mesh; (a) reference volume tracking solution on a 512×512 mesh, (b) volume tracking, (c) interface preserver and (d) transition algorithm.



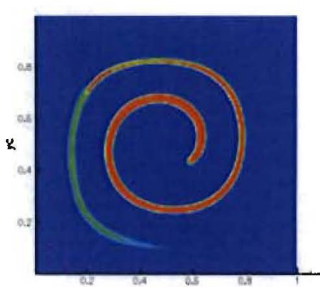
(a) Reference volume tracking solution on a 512×512 mesh



(b) Volume tracking (VOF)



(c) Interface preserver (IP)



(d) Transition algorithm (TRANS)

Figure 4: Volume fraction contours at time $t=4$ for the single vortex deformation flow field of period $T=8$ on a 128×128 mesh; (a) reference volume tracking solution on a 512×512 mesh, (b) volume tracking, (c) interface preserver and (d) transition algorithm.

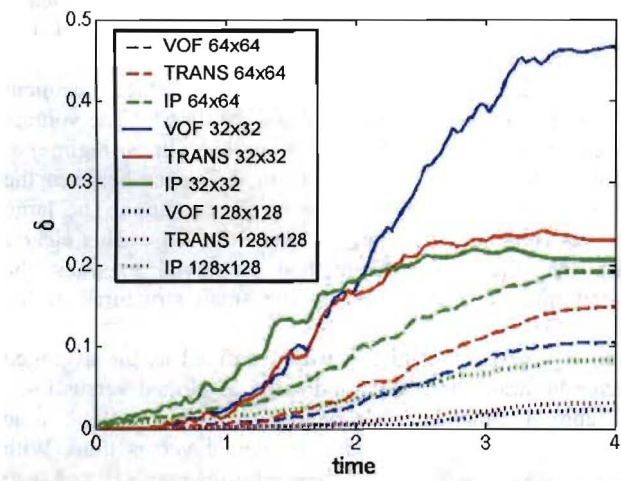


Figure 5: Volume fraction error versus time for the single vortex deformation flow field of period $T=8$ on the different mesh (32×32 , 64×64 and 128×128). The reference solution is obtained on a 512×512 mesh.

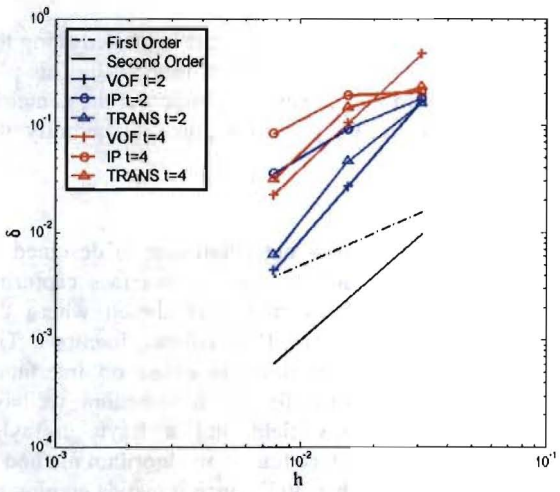
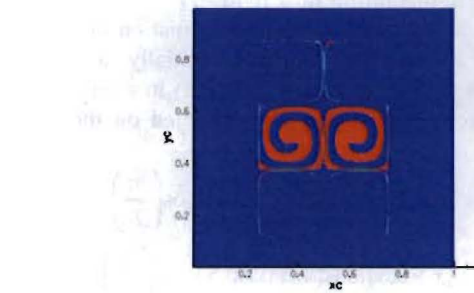
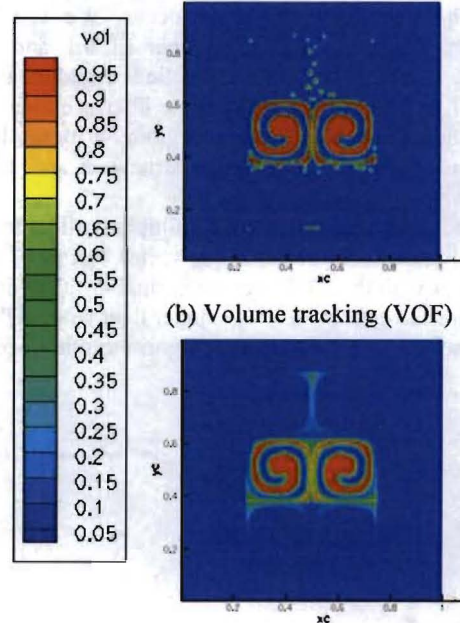


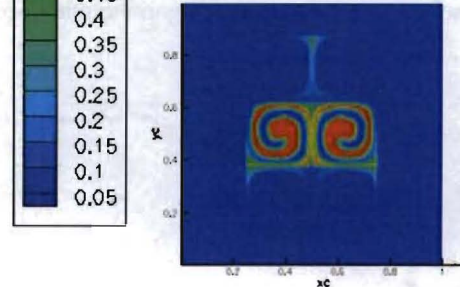
Figure 6: Volume fraction error versus mesh spacing (h) at time $t=2$ and $t=4$ for the single vortex deformation flow field of period $T=8$.



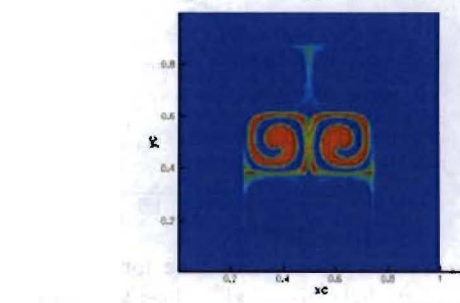
(a) Reference volume tracking solution on a 512×512 mesh



(b) Volume tracking (VOF)



(c) Interface preserver (IP)



(d) Transition algorithm (TRANS)

Figure 7: Volume fraction contours at time $t=1.5$ for the multiple vortex deformation flow field of period $T=4$ on a 128×128 mesh; (a) reference volume tracking solution on a 512×512 mesh, (b) volume tracking, (c) interface preserver and (d) transition algorithm.

Multiple vortices deformation flow field

We now consider a more stringent deformation flow field: the deformation by multiple vortices. Initially a circular interface of radius 0.15 is located at (0.5, 0.5) in a unit square domain. The velocity field (u_x u_y) is specified on the entire domain as:

$$\begin{aligned} u_x &= \sin(4\pi(x+0.5))\sin(4\pi(y+0.5))\cos\left(\frac{\pi t}{T}\right) \\ u_y &= \cos(4\pi(x+0.5))\cos(4\pi(y+0.5))\cos\left(\frac{\pi t}{T}\right) \end{aligned} \quad (4)$$

The simulation is run on a 128×128 mesh and until $T/2$ the time at which the maximum stretching occur. We use a constant time step based on a CFL number of 0.1 and a maximum velocity of unity. The volume fractions contours are shown in Figure 7. With the VOF method the interface breaks into multiple droplets in the thin filament regions. With the IP and the transition algorithm, the filament structures are still present but somewhat diffused.

The plot of the error metric, δ , for the multiple vortices test case is shown in Figure 8. As in the single vortex test case, at early times the error with the VOF method is smaller than with IP and at later times the error with IP is smaller than with VOF. This plot clearly shows that the transition algorithm minimizes the error.

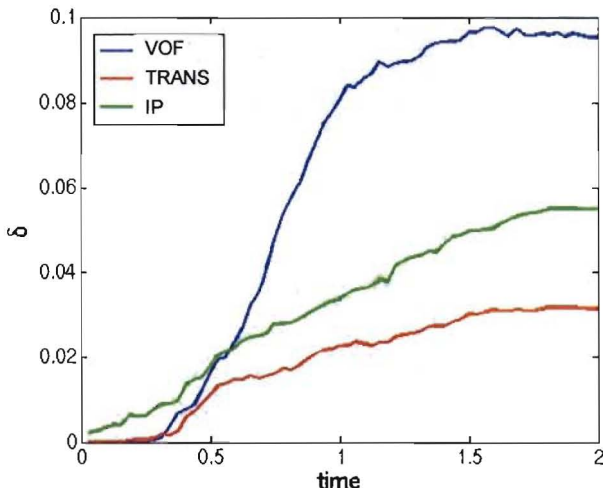


Figure 8: Volume fraction error versus time for the multiple vortex deformation flow field of period $T=4$ on the 128×128 mesh. The reference solution is obtained on a 512×512 mesh.

A FLUID FLOW EXAMPLE

We perform a fluid flow simulation of a single mode Rayleigh-Taylor instability to illustrate the effect of the material interface transition on the flow. For this case, we solve the incompressible Navier-Stokes equation using a pressure correction projection method (Francois et al., 2006). The computational domain is $[0,1] \times [-3,3]$, the mesh size is 50×300 .

The fluids are inviscid. The density ratio between the heavy and light fluids is 2 and the gravitational acceleration $g=0.1$ is acting downward.

In the linear regime, all numerical interface treatment methods predict the linear growth rate within 5%. The volume fraction contours are shown at late times (non-linear regime) in Figure 9 and in Figure 10. The main difference between the plots is seen in the region of the small structures. The large structures (bubble and spike) are about the same. This clearly shows that the numerical method employed to track the material interface affects mostly the small structures of the flow.

In Figure 11, the mixing width, defined as the averaged distance between the bubble and spike, is plotted versus time. In Figure 12 the interface velocity, defined as the time derivative of the mixing width, is plotted versus time. With VOF the mixing width is slightly greater than with IP and than with the transition algorithm at late times. The velocity plot confirms that the interface grows faster with the VOF method, since the velocity is greater in the plateau region of the plot. The faster growth of the mixing width with VOF is believed to come from the effect of the broken-up small structures on the flow.

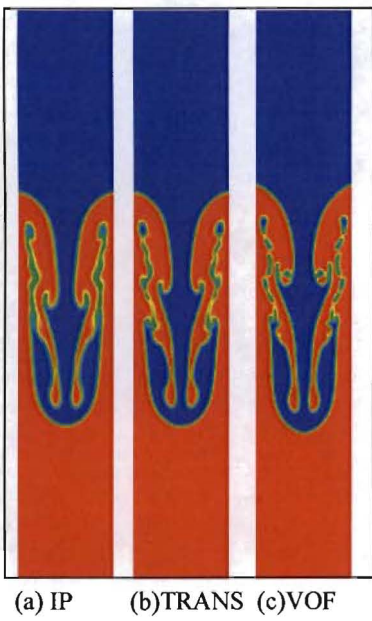
Finally in Figure 13, the density profile is plotted along the horizontal direction at the center ($y=0$) at time $t=20$. This plot gives some insight into the density distribution at the center in the mix region. Further analysis is required to quantify the numerical methods effect.

CONCLUDING REMARKS

We have presented a new algorithm that is designed to transition locally from volume tracking to interface capturing within a single fluid field Eulerian formulation where the material interfaces are represented by volume fractions. The transition criterion of the algorithm is based on interfacial curvature, a geometric measure. To test the algorithm, we have considered deformation flow field and a Rayleigh-Taylor instability. The material interface transition algorithm method is found to be more accurate than VOF since it avoids employing VOF in under-resolved regions. Further examination of the algorithm on the Rayleigh-Taylor instability will be made.

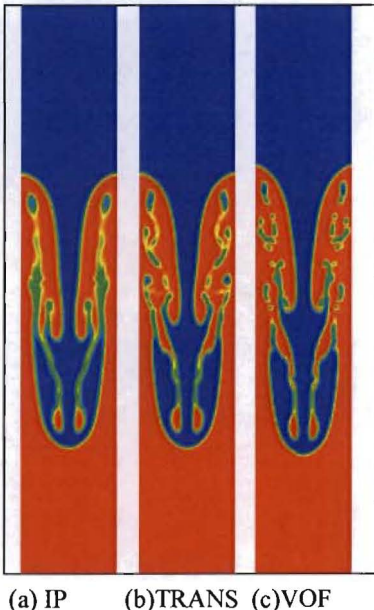
ACKNOWLEDGMENTS

This work was performed under the auspices of the National Nuclear Security Administration of the US Department of Energy at Los Alamos National Laboratory under Contract No. DE-AC52-06NA25396. This work is supported by the Advanced Simulation and Computing (ASC) program.



(a) IP (b) TRANS (c) VOF

Figure 9: Effect of material interface numerical treatment on single mode Rayleigh-Taylor instability in the non-linear regime. Volume fractions contours at $t=18$ with (a) interface preserver (IP), (b) transition algorithm (TRANS) and (c) volume tracking (VOF).



(a) IP (b) TRANS (c) VOF

Figure 10: Effect of material interface numerical treatment on single mode Rayleigh-Taylor instability in the non-linear regime. Volume fractions contours at $t=20$ with (a) interface preserver (IP), (b) transition algorithm (TRANS) and (c) volume tracking (VOF).

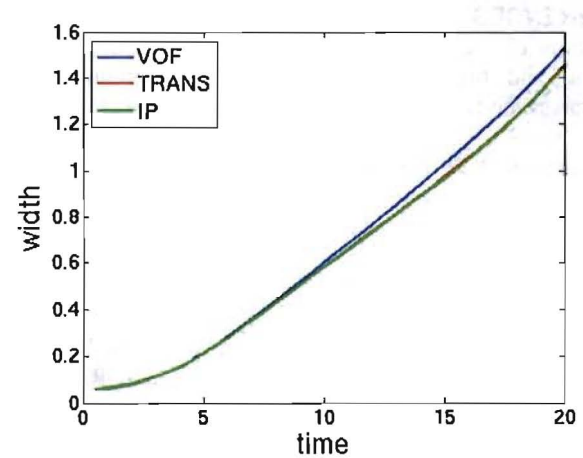


Figure 11: Rayleigh-Taylor instability mixing width growth.

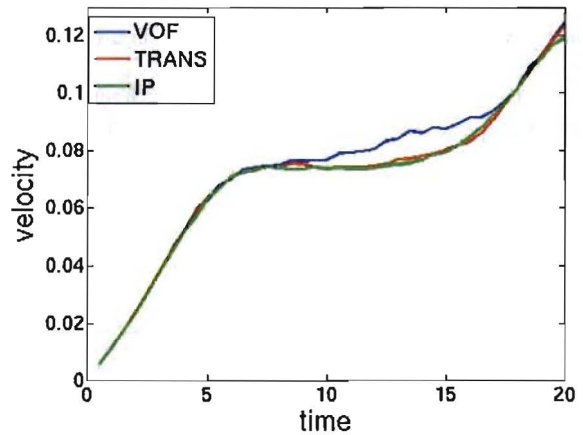


Figure 12: Rayleigh-Taylor instability mixing velocity versus time.

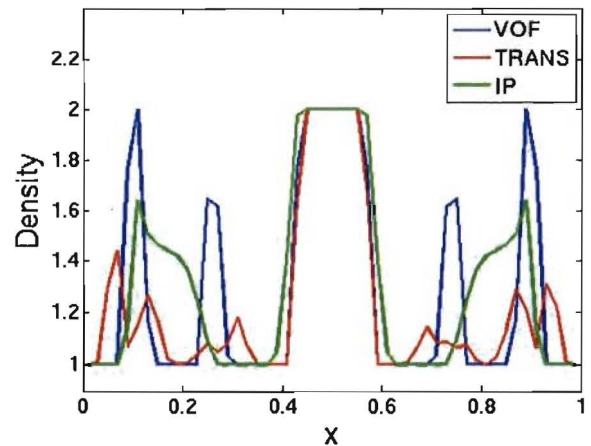


Figure 13: Density profile along the x direction at $y=0$ at $t=20$.

REFERENCES

Cerne G, Petelin S., Tiselj I., Coupling of the interface tracking and the two-fluid models for the simulation of incompressible two-phase flow, *J. Comp. Phys.*, 171, 776-804, 2001.

Cummins S.J., Francois M.M., Kothe D.B., Estimating curvature from volume fractions, *Computers and Structures*, 83, 425-433, 2005.

Dendy E.D., Rider W.J., The “Artificial Compression” technique in RAGE, Los Alamos Technical Report LA-UR-04-1971, 2004.

Dyadechko V. and Shaskov M., Moment-of-Fluid Interface Reconstruction, Los Alamos technical report LA-UR-05-7571, 2005.

Francois M.M., Cummins S.J., Dendy E.D., Kothe D.B., Sicilian J.M., Williams M.W., A balanced-force algorithm for continuous and sharp interfacial surface tension models within a volume tracking framework, *J. Comp. Phys.*; 213, 141-173, 2006.

Rider W.J., and Kothe D.B., Reconstructing volume tracking, *J. Comp. Phys.*, 141, 112-152, 1998.

Yang H.N., An artificial compression method for ENO Schemes. The slope modification method, *J. Comp. Phys.*, 89, 125-160, 1990.